

15. Crespo, J.L., Powers, T., Fowler, B., and Hall, M.N. (2002). The TOR-controlled transcription activators GLN3, RTG1, and RTG3 are regulated in response to intracellular levels of glutamine. *Proc. Natl. Acad. Sci. USA* 99, 6784–6789.
16. Hinnebusch, A.G. (2005). Translational regulation of GCN4 and the general amino acid control of yeast. *Annu. Rev. Microbiol.* 59, 407–450.
17. Kaeberlein, M., Powers, R.W., 3rd, Steffen, K.K., Westman, E.A., Hu, D., Dang, N., Kerr, E.O., Kirkland, K.T., Fields, S., and Kennedy, B.K. (2005). Regulation of yeast replicative life span by TOR and Sch9 in response to nutrients. *Science* 310, 1193–1196.
18. Steffen, K.K., MacKay, V.L., Kerr, E.O., Tsuchiya, M., Hu, D., Fox, L.A., Dang, N., Johnston, E.D., Oakes, J.A., Tchao, B.N., et al. (2008). Yeast life span extension by depletion of 60s ribosomal subunits is mediated by Gcn4. *Cell* 133, 292–302.
19. Borghouts, C., Benguria, A., Wawryn, J., and Jazwinski, S.M. (2004). Rtg2 protein links metabolism and genome stability in yeast longevity. *Genetics* 166, 765–777.

¹Department of Biochemistry, Albert Einstein College of Medicine, Morris Park Avenue, Bronx, NY 10461, USA, ²Buck Institute for Research on Aging, Redwood, Novato, CA 94945, USA, ³Guangdong Medical College, Dongguan, China.
*E-mail: marion.schmidt@einstein.yu.edu, bkennedy@buckinstitute.org

<http://dx.doi.org/10.1016/j.cub.2012.11.016>

Brain Mapping: The (Un)Folding of Striate Cortex

Neurons in the primary visual cortex of mammals form an orderly representation of the visual field. A recent study shows that the cortical folding pattern of the human brain accurately predicts not only the extent of this area, but also the location of cells that represent different points of visual space, leading to further considerations of the cortical mapping principles operating in related species.

Mark M. Schira¹,
Christopher W. Tyler²,
and Marcello G.P. Rosa³

The paper recently published in *Current Biology* by Benson *et al.* [1] is the latest in a long tradition of studies exploring the topographic organization of visual cortex, starting with the seminal studies of Tatsuji Inouye in 1906 [2] and Gordon Holmes in 1918 [3]. It has been long established that much of the primary visual area (area V1) of various primate species is located within a deep furrow, named the calcarine sulcus. Benson *et al.* [1] take the analysis of the coupling of structure and function in visual cortex significantly further, by providing strong evidence that the topology of the calcarine sulcus (a gross anatomical feature) and the map of the visual field in V1 (a functional measure, which correlates with visual acuity) are closely linked in the human brain.

Demonstration of this tight association allowed Benson *et al.* [1] to fit an algebraic model of the retinotopic map — a topographic description of which parts of the visual field are ‘seen’ by different neurons — to the cortical surface. Their innovative methodology allows the prediction of the parts of V1 that contain cells representing different parts of the visual field in other individuals, for which functional MRI

data are not available; this is an achievement that will most likely find application in other areas of brain

mapping. Many of the building blocks underlying the findings of Benson *et al.* [1] have been previously proposed, including the automatic estimation of V1 boundaries in individuals [4], and a precise algebraic model of the visual field map in human V1 [5]. However, putting these elements together into an integrated whole, including new methods for quantifying and visualizing structural–functional relationships, has provided a much more compelling argument.

The strikingly systematic relationship between structural and functional

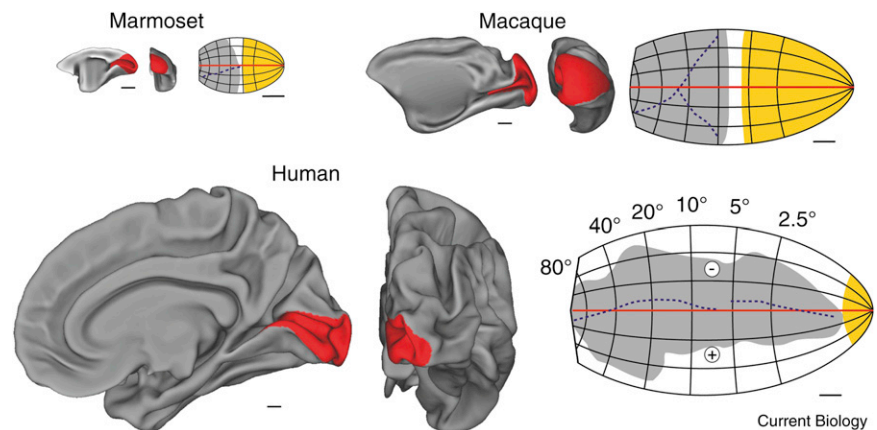


Figure 1. Comparison of the extent and retinotopic maps of area V1 in three primate species with very different brain sizes (marmoset monkey, macaque monkey and human).

Each panel shows medial (left) and posterior (center) views of partially ‘inflated’ right hemispheres of the brains of the three species, based on MRI reconstructions of the middle layers of the cortex (prepared with CARET [19]). The location of area V1 is indicated in red. On the right are two-dimensional models of the retinotopic organization of V1, fitted to high-resolution data as described elsewhere [13,16]. The map of human V1 indicates the positions of imaginary lines that join the locations of neurons representing parts of the visual field located at different distances from the point of fixation (2.5°, 5° and so on), as well as regions representing the upper (+) and lower (-) parts of the visual field, and the representation of the horizontal meridian (red line). The grey region indicates the part of V1 that is buried within the calcarine sulcus, and the yellow region indicates the part that is exposed on the surface of the occipital lobe (white indicates regions that are exposed on the mesial surface of the brain). Corresponding landmarks are shown for macaque and marmoset monkey. Whereas in the human brain there is good correspondence between the representation of the horizontal meridian and the main fold of the calcarine sulcus (dashed line), this simple relationship is not present in marmoset and macaque. This occurs despite the striking similarity in retinotopic organization, across brains that differ over 100 times in mass. Scale bars in all panels = 5 mm.

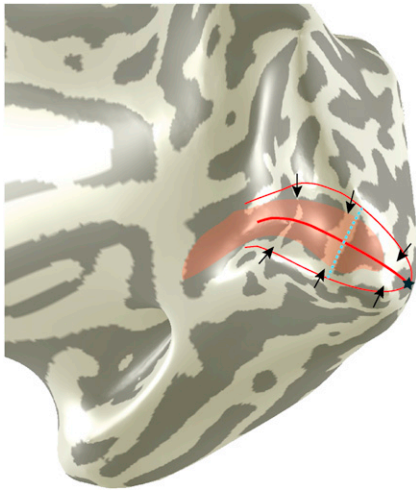


Figure 2. ‘Rungs’ across the calcarine sulcus may help predict eccentricity mapping.

An inflated three-dimensional reconstruction of the gray-white matter boundary from one human subject. Light and dark gray patches illustrate the pattern of gyri and sulci, respectively. The transparent red overlay signifies the calcarine sulcus, the red lines illustrate the horizontal and vertical meridian representations in V1. Finally the star denotes the representation of the fixation point, and the arrows point to small internal gyri, which run orthogonal to the calcarine sulcus like the rungs of a ladder. We found the position of these ‘rungs’ very reliable across subjects (9 out of 10 subjects for both hemispheres), reliably coinciding with the 0.5 and 5° (green dotted line = 5°) isoeccentricity lines. The third pair of arrows points to a third, less pronounced rung that is present in some individuals, coinciding approximately with the 20° isoeccentricity line.

features in human V1 raises questions about the underlying causality, possibly in the form of morphogenetic interactions between developing connectivity and the mechanics of cortical folding [6]. Here, the findings of Benson *et al.* [1] may prompt new studies using mathematical models to explore the development of relationships between structure and function in cortical morphogenesis. For example, the tight spatial linkage between the fundus of the calcarine sulcus and the representation of the horizontal meridian (the imaginary line across our fixation point dividing our visual fields into upper and lower halves) that has been demonstrated by the authors appears to be, according to current knowledge, specific to human brains (Figure 1). In most monkeys, and in the related prosimians, this fold divides V1 into unequal halves [7–10] and the part inside the calcarine

shows little tendency for the horizontal meridian to conform to the fold of the fundus.

The notable differences in V1 folding across different species raise challenging questions for the understanding of its morphogenesis, as the relative invariance of V1 within species lends weight to the view that the outline of this area is to a large extent genetically determined, as suggested by molecular biological studies of corticogenesis [11]. In comparison, the boundaries and topographic maps in other areas are likely to mature later, partially under ‘instructions’ conveyed by V1 projections, and constrained by the need to keep map continuity between adjacent cells. This iterative process is hypothesized to allow more degrees of freedom, which translate into individual variability [12].

It has been long recognized that the boundaries of V1 in human are well co-localized with the lips of the calcarine sulcus. The work by Benson *et al.* [1] shows that the internal folding pattern along the length of this sulcus also provides practical landmarks for other features of the map. They demonstrate a strong correspondence between the representation of the horizontal meridian and the fundus of the calcarine sulcus. Moreover, they use a template map to help predict the location of other parts of the visual field, for example those that are immediately above or below this meridian, or near the vertical meridian (another imaginary line across the fixation point, which divides the visual field into left and right halves).

We would like to take this concept further by suggesting that there are, in most individuals, visible landmarks that may provide anchors for another dimension of the mapping — eccentricity (distance from the fixation point). These are characteristic folds running across the width of the calcarine sulcus, forming ‘rungs’ that run between its upper and lower lips. Encouraged by the results from Benson *et al.* [1], we re-examined retinotopic mapping data in humans [13], finding that these rungs tend to be located at reproducible locations in different individuals, corresponding to the representation of eccentricities 0.5

and 5° of visual angle from the fovea, and perhaps a third one around 20° (Figure 2). These features may help constrain algebraic models of the visual field representation [5], thus providing a more complete prediction of the functional mapping solely from anatomical data. Exploring the retinotopic consistency of these internal landmarks has the potential to provide surgeons and experimenters with further ‘signposts’ to navigate the brain, including, for example, the positioning of prosthetic devices aimed at eliciting artificial vision in the blind [14].

Finally, the work of Benson *et al.* [1] also raises a number of other questions that will stimulate further research on the topographic organization of V1, and its relationship to visual acuity. One potentially controversial observation is that their average V1 map shows a strong overrepresentation of the horizontal versus the vertical meridian. This feature of the proposed human V1 template is peculiar because it is not apparent in previous work addressing this issue in different primate species [7,13,15–17]. The authors acknowledge this in their supplementary materials, proposing that “*At least some of this variation in areal magnification across polar angle is a consequence of the cortical inflation process and projection to a two-dimensional surface*”. This is an important point, because without this context their results could be interpreted as predicting substantially greater visual acuity for objects located near the horizontal than the vertical meridian (but at similar distances from the fovea). If further work confirms that the normalization and flattening procedures introduce a systematic distortion of the V1 topography, this would indicate an inherent (Gaussian) curvature in the intrinsic shape of V1, with a shape more similar to a rugby ball rather than flat. Previous detailed analyses suggested that there is little systematic curvature in human V1 [15], and accordingly current mathematical models of the V1 map are strictly two-dimensional [5,18]. In the light of the results from Benson *et al.* [1], the degree of local V1 curvature and its integration into accurate conceptual models of V1 deserves reinvestigation, ideally using high-resolution techniques.

References

1. Benson, N.C., Butt, O.H., Datta, R., Radoeva, P.D., Brainard, D.H., and Aguirre, G.K. (2012). The retinotopic organization of striate cortex is well predicted by surface topology. *Curr. Biol.* 22, 2081–2085.
2. Inouye, T. (1906). Visual disturbances following gunshot wounds of the cortical visual area by Tatsuji Inouye (translated by M. Glickstein & M. Fahle). *Brain* 123 (special suppl.), 1–100.
3. Holmes, G. (1918). Disturbances of visual orientation. *Br. J. Ophthalmol.* 2, 506–516.
4. Hinds, O., Polimeni, J.R., Rajendran, N., Balasubramanian, M., Amunts, K., Zilles, K., Schwartz, E.L., Fischl, B., and Triantafyllou, C. (2009). Locating the functional and anatomical boundaries of human primary visual cortex. *Neuroimage* 46, 915–922.
5. Schira, M.M., Tyler, C.W., Spehar, B., and Breakspear, M. (2010). Modeling magnification and anisotropy in the primate foveal confluence. *PLoS Comput. Biol.* 6, e1000651.
6. Van Essen, D.C. (1997). A tension-based theory of morphogenesis and compact wiring in the central nervous system. *Nature* 385, 313–318.
7. Gattass, R., Sousa, A.P., and Rosa, M.G. (1987). Visual topography of V1 in the Cebus monkey. *J. Comp. Neurol.* 259, 529–548.
8. Fritsches, K.A., and Rosa, M.G. (1996). Visuotopic organisation of striate cortex in the marmoset monkey (*Callithrix jacchus*). *J. Comp. Neurol.* 372, 264–282.
9. Rosa, M.G., Casagrande, V.A., Preuss, T., and Kaas, J.H. (1997). Visual field representation in striate and prestriate cortices of a prosimian primate (*Galago garnettii*). *J. Neurophysiol.* 77, 3193–3217.
10. Gattass, R., Gross, C.G., and Sandell, J.H. (1981). Visual topography of V2 in the macaque. *J. Comp. Neurol.* 201, 519–539.
11. Donoghue, M.J., and Rakic, P. (1999). Molecular evidence for the early specification of presumptive functional domains in the embryonic primate cerebral cortex. *J. Neurosci.* 19, 5967–5979.
12. Rosa, M.G., and Tweeddale, R. (2005). Brain maps, great and small: lessons from comparative studies of primate visual cortical organization. *Phil. Trans. R. Soc. Lond. B* 360, 665–691.
13. Schira, M.M., Tyler, C.W., Breakspear, M., and Spehar, B. (2009). The foveal confluence in human visual cortex. *J. Neurosci.* 29, 9050–9058.
14. Torab, K., Davis, T.S., Warren, D.J., House, P.A., Normann, R.A., and Greger, B. (2011). Multiple factors may influence the performance of a visual prosthesis based on intracortical microstimulation: nonhuman primate behavioural experimentation. *J. Neural. Eng.* 8, 035001.
15. Schira, M.M., Wade, A.R., and Tyler, C.W. (2007). Two-dimensional mapping of the central and parafoveal visual field to human visual cortex. *J. Neurophysiol.* 97, 4284–4295.
16. Chaplin, T.A., Yu, H.H., and Rosa, M.G.P. (2012). Representation of the visual field in the primary visual area of the marmoset monkey: magnification factors, point-image size and proportionality to retinal ganglion cell density. *J. Comp. Neurol.* <http://dx.doi.org/10.1002/cne.23215>.
17. Adams, D.L., and Horton, J.C. (2003). A precise retinotopic map of primate striate cortex generated from the representation of angioscotomas. *J. Neurosci.* 23, 3771–3789.
18. Polimeni, J.R., Balasubramanian, M., and Schwartz, E.L. (2006). Multi-area visuotopic map complexes in macaque striate and extra-striate cortex. *Vision Res.* 46, 3336–3359.
19. Van Essen, D.C., Drury, H.A., Dickson, J., Harwell, J., Hanlon, D., and Anderson, C.H. (2001). An integrated software suite for surface-based analyses of cerebral cortex. *J. Am. Med. Inform. Assoc.* 8, 443–459.

¹Neuroscience Research Australia, Randwick, NSW, Australia & School of Psychology, University of Wollongong, Wollongong, NSW, Australia, ²Smith-Kettlewell Brain Imaging Center, Smith-Kettlewell Eye Research Institute, San Francisco, CA, USA, ³Department of Physiology and Monash Vision Group, Monash University, Melbourne, VIC, Australia.
E-mail: mark.schira@gmail.com, cwt@ski.org, marcello.rosa@monash.edu

<http://dx.doi.org/10.1016/j.cub.2012.11.003>

Intracellular Transport: New Tools Provide Insights into Multi-motor Transport

Teams of kinesin and dynein motors drive bidirectional transport of intracellular cargoes along the microtubule cytoskeleton. How do opposite-polarity motors interact to achieve targeted trafficking? A new study uses tools from synthetic biology to probe collective motor function.

Adam G. Hendricks¹,
Alison E. Twelvetrees^{1,2},
and Erika L.F. Holzbaur¹

Many intracellular cargoes move bidirectionally along the microtubule cytoskeleton, transported by teams of kinesin and dynein motors [1]. Kinesin drives motility towards microtubule plus ends, while dynein moves towards the minus end. The collective function of motor teams allows cargoes to move bidirectionally over large distances. This long-range transport is vital for extended, polarized cells such as neurons. Indeed, defects in microtubule motors cause neurodegenerative disease, and impaired axonal transport has been identified in models of amyotrophic lateral sclerosis, and Alzheimer's and

Huntington's diseases [2]. Despite its fundamental importance, an understanding of how interactions among motors on a cargo modulate their function to achieve targeted trafficking in the cell remains poorly understood.

Several mechanisms have been proposed to describe bidirectional transport. One hypothesis is that directional switches are the result of a regulatory event [1]. Alternatively, bidirectional motility may result from a stochastic tug-of-war between opposite polarity motors bound to the same cargo. In this case, switching is a consequence of the force-dependent dissociation kinetics of the motors, in the absence of regulation [3]. These mechanisms are not mutually exclusive, and both are likely to

contribute to the motility of intracellular cargoes [4].

Diverse approaches have been used to elucidate the mechanisms of multi-motor transport, ranging from *in vitro* reconstitution using purified motors bound to latex beads to high-resolution tracking of endogenous cargoes moving in the cell (Figure 1). In a recent paper published in *Science*, Derr *et al.* [5] implement a novel synthetic biology approach. The authors construct a scaffold using DNA origami — a technique that allows the creation of complex three-dimensional structures from DNA [6]. Motor proteins can be specifically attached to these artificial scaffolds via strands of complementary DNA, and in this way the number and type of motors can be tightly controlled. Derr *et al.* [5] use these scaffolds to examine motility by teams of dynein and kinesin motors. In agreement with previous work [7,8], the authors find that the run length of the cargoes increases with the number of motors, while velocity is largely unaffected [9]. They next examine teams of dynein and kinesin bound to the same cargo. Although the human kinesin-1 and yeast cytoplasmic dynein motors used in this study have similar unitary stall forces, a few dynein motors